Electronic Supplementary Material (ESI) for CrystEngComm.

Supporting Information for

Morphological and Orientational Diversity of $LiFePO_4$ Crystallites: Remarkable Reaction Path Dependence in Hydrothermal/Solvothermal Syntheses

Zhaojin Li,[†,§] Kongjun Zhu,[‡] Jialin Li[†], and Xiaohui Wang[†,*]

[†]Shenyang National Laboratory for Materials Science, Institute of Metal Research, Chinese Academy of Sciences, 72 Wenhua Road, Shenyang 110016, China

[‡]State Key Laboratory of Mechanics and Control of Mechanical Structures, Nanjing University of Aeronautics and Astronautics, Nanjing 210016, China

[§]University of Chinese Academy of Sciences, Beijing 100039, China

S.1. Transformation from Li_3PO_4 to $LiFePO_4$ (LFP) indicated by Raman Spectroscopy

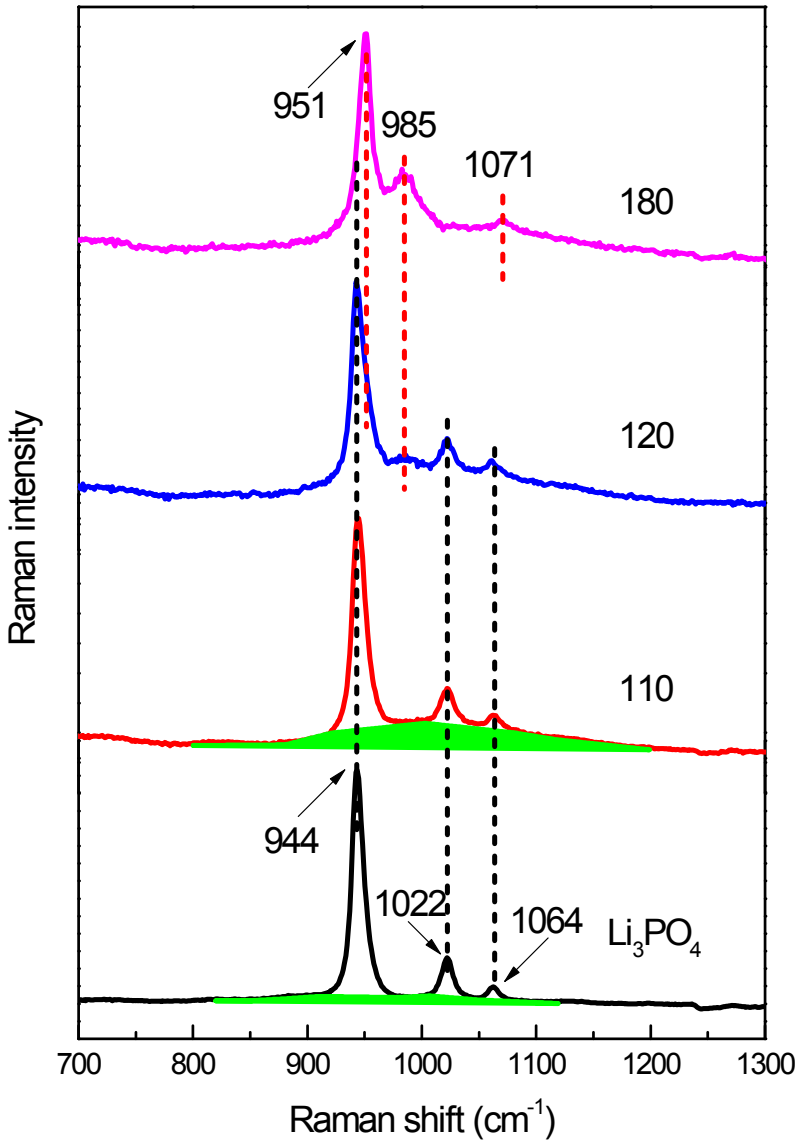

Figure S1. Raman spectra of Li_3PO_4 and those heated at various temperatures under the S–UR condition, indicating the presence of a profound background for the sample (S–UR–(110)). This background is an indicator of amorphization during the in situ transformation of Li_3PO_4 to LFP. Black dashed lines and the red ones correspond to the Raman bands of Li_3PO_4 and LFP, respectively.

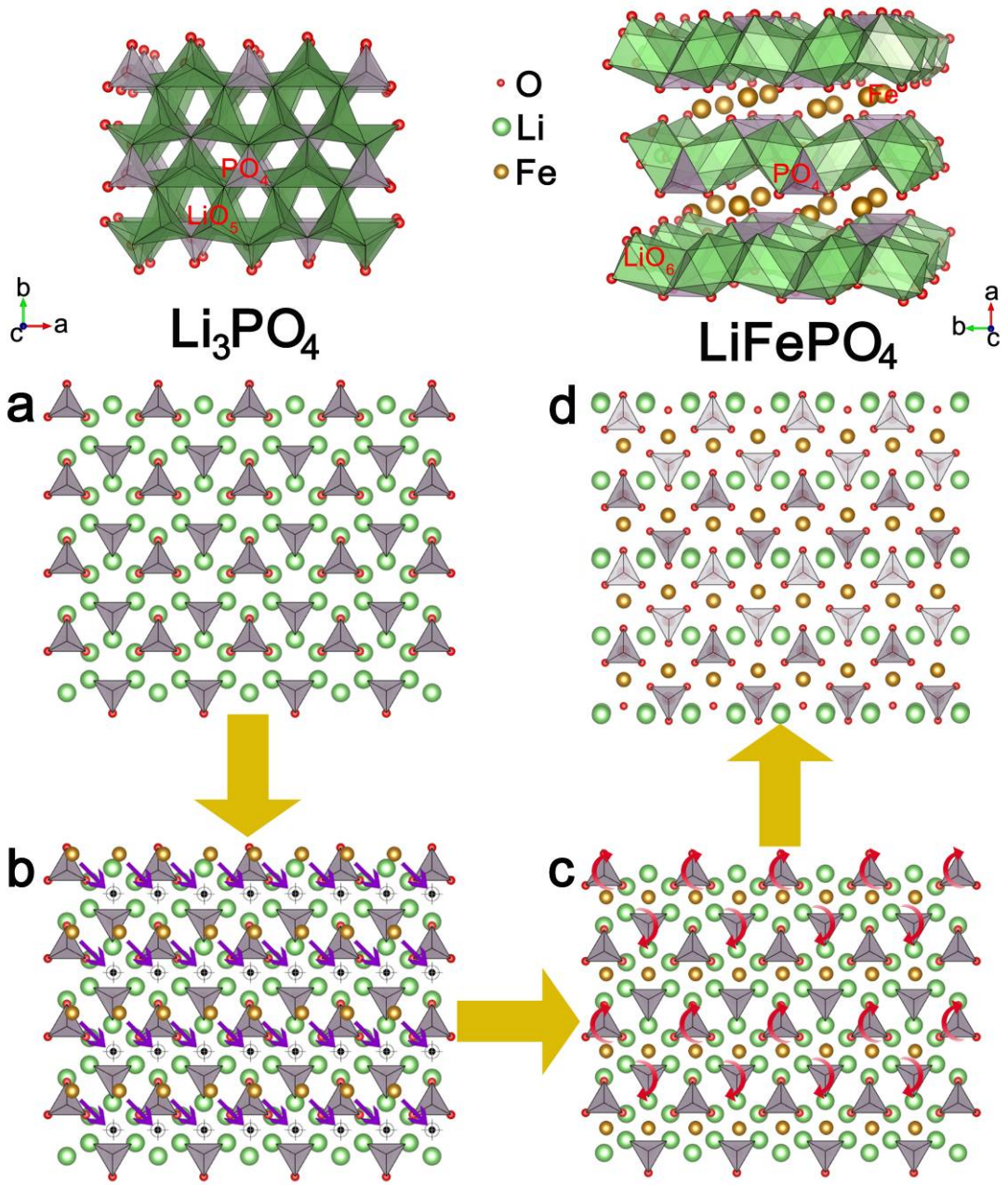

Figure S2. Schematic illustration showing the transformation from Li_3PO_4 to LFP. In the crystal of Li_3PO_4, each PO_4 tetrahedron is surrounded by nine LiO_5 hexahedra of which three are edging-sharing and six are corner-sharing. LFP crystallizes in the olivine structure. It is built up of PO_4 tetrahedra, with the Fe^{2+} cations occupying corner-shared octahedral positions, and the Li^+ cations located in chains of edge-sharing octahedra. Due to the difference in configuration of PO_4 tetrahedra in Li_3PO_4 and LFP, transition of Li_3PO_4 into LFP involves the reposition of PO_4 tetrahedra upon the incorporation of Fe^{2+} cations. The reposition predominantly includes the rotation of the PO_4 tetrahedra that are the skeleton of Li_3PO_4. As a result, the crystal of Li_3PO_4 collapsed, giving rise to an amorphization process, as indicated by the Raman spectra (Figure S1). With the reconstruction as shown in Figure S2 c, the structure of LFP is established.

S.2. XRD patterns of the intermediate phases by using ethanol, glycerol and polyethylene glycol 200 as solvents.

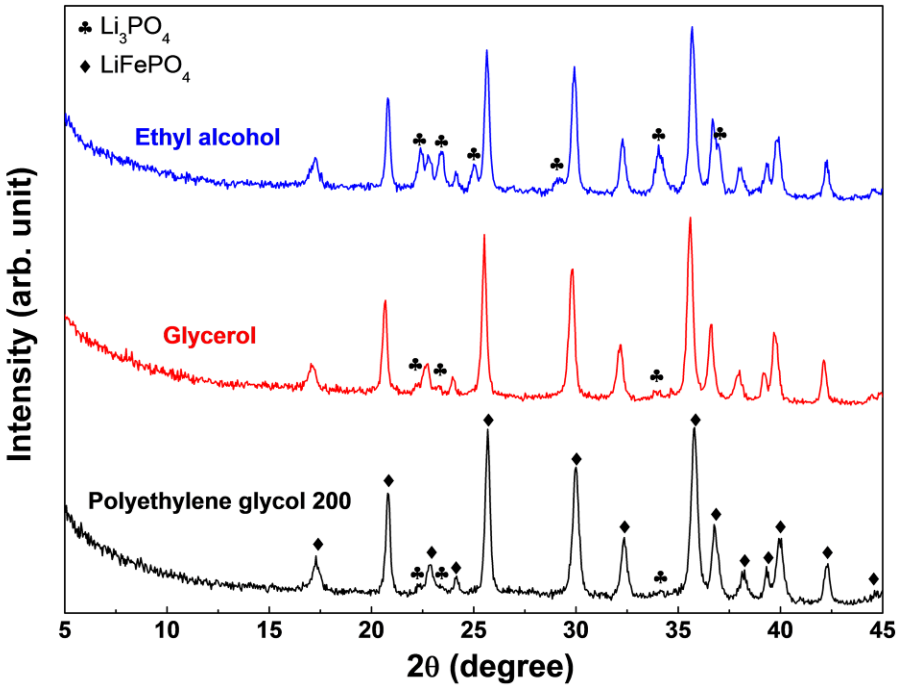

Figure S3. XRD patterns of samples heated up to 120 °C using ethanol, glycerol and polyethylene glycol 200 as solvents. Note that no other phases but Li_3PO_4 and LFP are identified.

S.3. Electrochemical Performance.

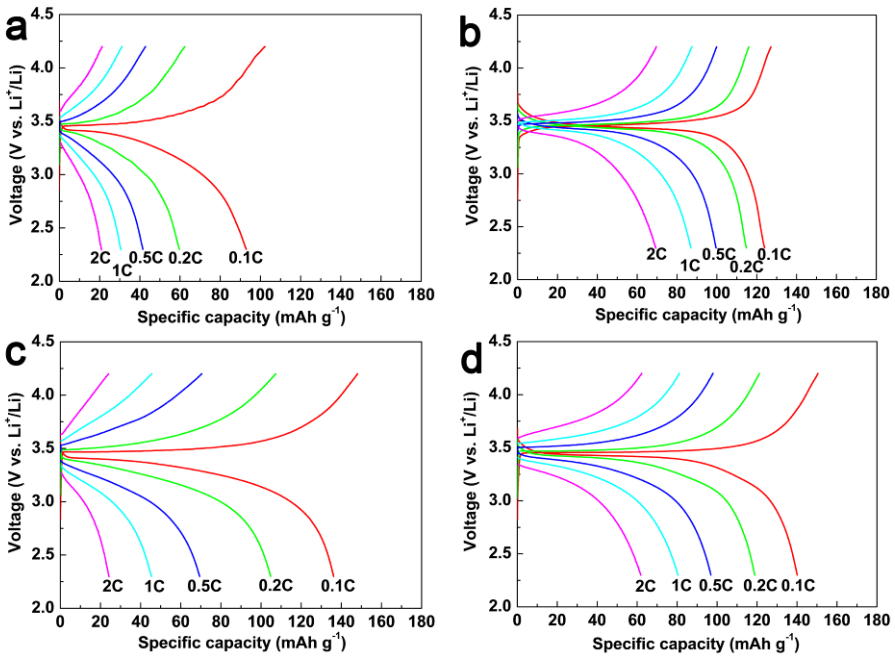

Figure S4. Electrochemical performances of bare LFP particles. The electrodes were prepared by mixing 80 wt% bare LFP, 15 wt% acetylene black, and 5 wt% poly(vinylidene fluoride). (a) H–UR (LFP), the electrode delivers a specific capacity of ca. 93.0, 59.7, 41.5, 30.5 and 20.9 mA h g^{-1} at 0.1, 0.2, 0.5, 1 and 2 C, respectively. (b) S–UR (LFP), the electrode delivers a specific capacity of ca. 124.0, 114.8, 99.6, 87.0 and 69.4 mA h g^{-1} at 0.1, 0.2, 0.5, 1 and 2 C, respectively. (c) H–EP (LFP), the electrode delivers a specific capacity of ca. 136.2, 104.8, 69.4, 45.4 and 24.3 mA h g^{-1} at 0.1, 0.2, 0.5, 1 and 2 C, respectively. (d) S–EP (LFP), the electrode delivers a specific capacity of ca. 140.1, 118.9, 96.9, 80.4 and 61.6 mA h g^{-1} at 0.1, 0.2, 0.5, 1 and 2 C, respectively.

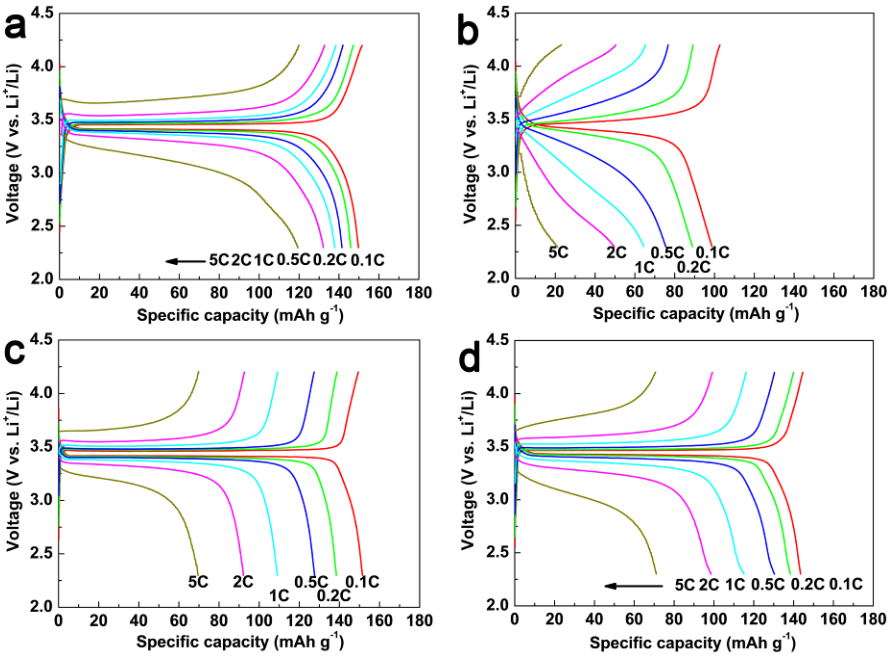

Figure S5. Electrochemical performances of LFP/C composites in the absence of conducting agent (acetylene black). The electrodes were prepared by mixing 90 wt% cathode composite, 10 wt% poly(vinylidene fluoride). (a) H–UR (LFP/C), the electrode delivers a specific capacity of ca. 149.7, 145.9, 141.5, 137.9, 132.1 and 119.4 mA h g^{-1} at 0.1, 0.2, 0.5, 1, 2 and 5 C, respectively. (b) S–UR (LFP/C), the electrode delivers a specific capacity of ca. 98.7, 88.9, 75.5, 64.3, 49.7 and 21.2 mA h g^{-1} at 0.1, 0.2, 0.5, 1, 2 and 5 C, respectively. (c) H–EP (LFP/C), the electrode delivers a specific capacity of ca. 151.5, 138.5, 127.7, 109.2, 92.2 and 69.6 mA h g^{-1} at 0.1, 0.2, 0.5, 1, 2 and 5 C, respectively. (d) S–EP (LFP/C), the electrode delivers a specific capacity of ca. 143.5, 138.4, 130.4, 115.1, 98.6 and 71 mA h g^{-1} at 0.1, 0.2, 0.5, 1, 2 and 5 C, respectively.

S.4. SEM images of the LFP/C composites.

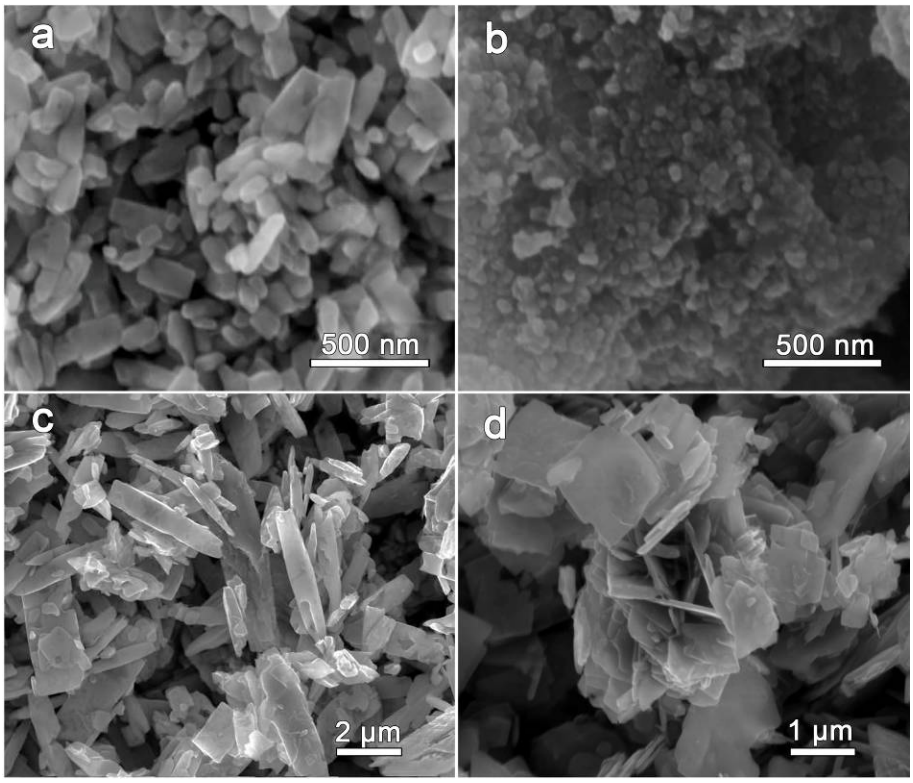

Figure S6. SEM images of the LFP/C composites, indicating that the morphologies of the synthesized LFP crystallites are well preserved with carbon coating at 650 °C. (a) H–UR (LFP/C), (b) S–UR (LFP/C), (c) H–EP (LFP/C), and (d) S–EP (LFP/C)

S.5. FTIR spectra of the LFP/C composites.

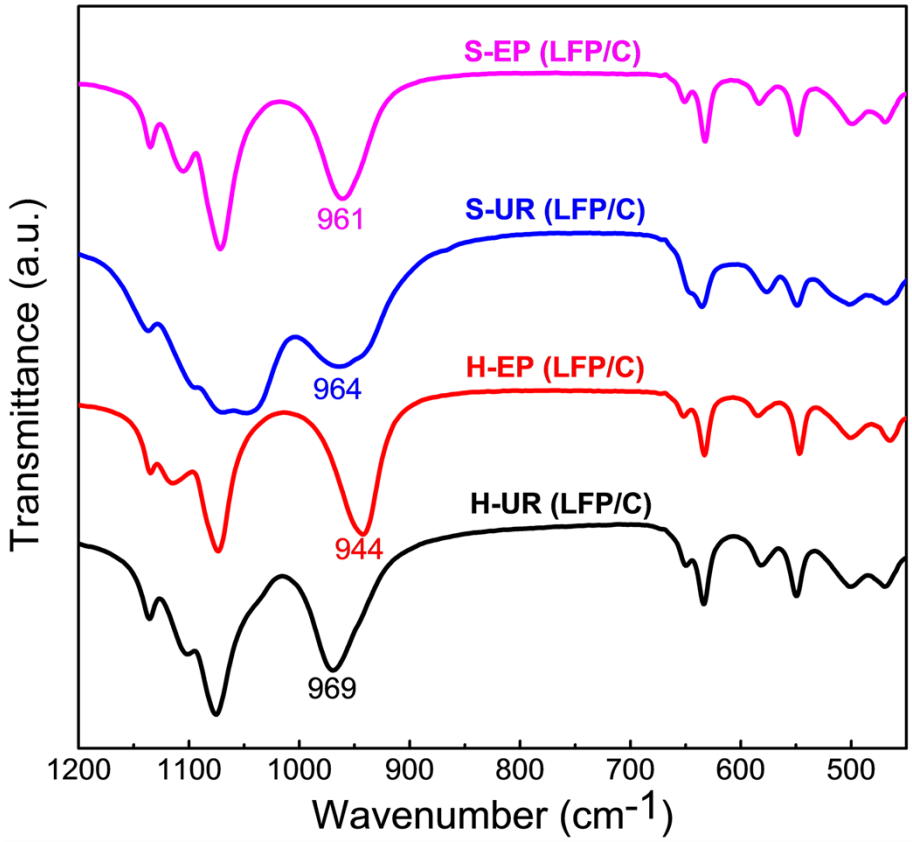

Figure S7. FTIR spectra of the LFP/C composites.